Effect of Pumped Gas Reflux on Divertor Operation in ITER

A.S. Kukushkin[1], H.D. Pacher[2], V. Kotov[3], D. Reiter[3], D. Coster[4], G.W. Pacher[5]

[1] ITER IT, Garching, Germany
[2] INRS-EMT, Varennes, Québec, Canada
[3] FZ Jülich, Jülich, Germany
[4] Max-Planck Institut für Plasmaphysik, Garching, Germany
[5] Hydro-Québec, Varennes, Québec, Canada

E-mail contact of the main author: Andrei.Kukushkin@iter.org

Abstract. The paper describes the latest results of B2-Eirene modelling of ITER divertor operation. The operational window is further explored with an improved model of the neutral transport, the effect of gas leaks between the divertor cassettes is assessed, and the sensitivity of the results to the details of the divertor geometry and arrangement of gas puff is analysed.

1. Introduction

The presence of gas leaks through the divertor structures is an important aspect of ITER divertor design which has not yet been addressed in modelling studies. Indeed, the ITER divertor consists of 54 modules (cassettes) [1] which are to be assembled remotely inside the vacuum vessel. For technical reasons the poloidal gaps between the cassettes can not be sealed perfectly, and therefore unintended particle fluxes will occur between the divertor and the gas volume inside the cassette. The primary aim of this paper is to explore the effect of these fluxes on the performance of the ITER divertor. Furthermore, the sensitivity of the divertor operation to the position of the separatrix strike points on the targets and to the detail of the target shape and arrangement of gas puff is re-considered by means of the recently improved model [2] now routinely used for ITER analysis.

In the present study, we use the B2-Eirene code package version solps4.2 [2] with a non-linear model of neutral particle transport, which includes neutral-neutral and molecule-ion collisions. For the present study, we take the whole inner surface of ITER to be covered by carbon. The other model assumptions are those of [2]. In particular, we fix the plasma power entering the scrape-off layer (SOL) at 100 MW, fix the D ion flow from the core across the core-edge interface (CEI) at 17 $Pa{\cdot}m^3s^{-1}$, and vary the density by varying the gas puffing flux. The D_2 gas is puffed from the top (except for one variant), and pumped via the duct in the private-flux region (PFR) at the bottom of the chamber and via the cassette leaks. The plasma consists of D (representing both D and T), He, and C ions and atoms, and D_2 molecules.

The model taking into account the gas leaks between the divertor components is described in section 2, and results upon application to ITER are shown in section 3. The sensitivity of the modelling results to the shape of the divertor bottom and to the shift of the separatrix strike points on the targets are analysed in sections 4 and 5, the effect of mid-plane gas puff in section 6, and section 7 presents the conclusions.

2. Model of Gas Leaks in the Divertor

A cartoon of the particle flows in the divertor region is shown in Fig. 1. Here Γ_p means the flux to the pump, Γ_d the flux from the PFR into the duct, Γ_i the ion flux from the core to the scrape-off layer (SOL), Γ_n the neutral flux from the SOL to the core, Γ_c the core fuelling (for D) or production (for He). We model two kinds of leaks: from the cassette body to the SOL at

the baffle, Γ_b, and from the PFR to the cassette body at the "V's" in the divertor corner, Γ_v. The leaks are characterized by the gas conductance of corresponding gaps and the pressure difference. In our calculations, we do not model the neutral transport within the cassette body – modelling of this essentially three-dimensional volume would be computationally too expensive. Instead we specify additional gas puffing for the reflux at the baffle, Γ_b, and extra particle absorption (equivalent to pumping) at the "V", Γ_v. This scheme is justified by the observation that the gas pressure at the "V"s, p_v, is always considerably (factor 3 or more) higher than the pressure at the duct entrance, p_d, which is higher than the pressure inside the cassette body, p_c, which is in turn higher than the pressure at the baffle p_b.

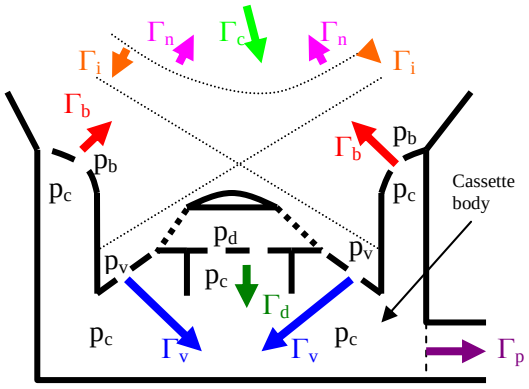

Fig. 1. Schematic of the particle flows in the divertor region of ITER

In these conditions, a natural measure for the leaks through the "V"s is the ratio of the "reduced" pumping speed through the "V" surface to the sum of this pumping speed and that through the pumping duct. Here, "reduced" means the pumping speed estimated for the same gas temperature, so that the leakage factor $\alpha_v = (\xi_v \cdot A_v) / (\xi_d \cdot A_d + \xi_v \cdot A_v)$ [3] where ξ stands for the particle absorption at, and A for the area of, the corresponding surface. For the most of runs with the V-leak, $\alpha_v = 0.2$ was selected, which results in $\Gamma_v \sim \Gamma_d$ because p_v is several times p_d. Typical gap sizes for the ITER design without specific sealing measures are 54 toroidal gaps, 2 m long, 5 mm wide and 5 cm deep [4]. Accurate evaluation of α_v would require Monte Carlo neutral calculations, but, taking $p_c << p_v$, one can estimate a value $\alpha_v \sim 0.04$ [4, 5]. Selecting $\alpha_v = 0.2$, we therefore ascertain that the effect of these leaks is bracketed by the calculations. If sealing measures reduced the gap size to 1 mm, use of expressions such as those of [5] would indicate that the gaps would then be entirely negligible.

A natural measure of the leak from the cassette to the SOL through the baffle is the ratio $\alpha_b = \Gamma_b / (\Gamma_b + \Gamma_p)$ (note that there is no singularity when $\Gamma_p = 0$). If the gas pressure inside the cassette body p_c were uniform, this would be the ratio of the gas conductance of the leaks in the baffle to the sum of this conductance with that of the downpipe to the pump. The desired value of α_b is achieved in the course of a calculation via adjustment of the additional puffed flux Γ_b. The value $\alpha_b = 0.5$, that is, $\Gamma_b = \Gamma_p$, corresponds to the cassette design without sealing [4]. In the model, the reflux is usually distributed uniformly over the baffle (inner and outer) region, and calculations show a weak sensitivity of the results to this distribution.

Since the atomic masses of He and D_2 are the same, and they are in equilibrium with the walls within the cassette body, it is reasonable to assume that the pressure distribution there is the same for He and D_2. Then for each plasma component

$$\Gamma_p = \Gamma_d + \Gamma_v - \Gamma_b, \quad \Gamma_b = \alpha_b(\Gamma_p + \Gamma_b) = \alpha_b(\Gamma_d + \Gamma_v), \quad \Gamma_p = (1-\alpha_b)(\Gamma_d + \Gamma_v) \qquad (1)$$

The helium ion flux Γ_i from the core to the SOL, equal to the sum of the fusion He production rate in the core and the neutral flux from the SOL to the core, $\Gamma_i = \Gamma_c + \Gamma_n$, is specified at the CEI, and this value is adjusted in the course of the calculation.

3. Effect of the Leaks on the Divertor Performance

In order to determine the effect of particle reflux, we did three density scans for the values of

α_b = 0, 0.15, and 0.5, keeping α_v = 0.2. In the figures, the dashed lines marked "fit" indicate the variation of the parameters established in previous studies using the linear model, and further investigated with the nonlinear neutral model [6], and the position of the transition to detached operation of the inner divertor is also indicated (see [6]). Fig. 2 shows the variation of peak power load of the target q_{pk} with the neutral pressure in the PFR. No significant change occurs when α_b is varied – that is, the power load remains strongly correlated with the neutral pressure in the PFR, as in [2, 7, 6]. The maximum of the plasma temperature along the targets decreases (Fig. 2b and 2c). This occurs because the additional throughput through the "V"s (even in the absence of reflux) at the same average neutral pressure, p_{DT}, at the plasma interface requires higher neutral pressure inside the divertor plasma, and this leads to a lower plasma temperature at the target. When the reflux neutrals are introduced (variation of α_b from 0 to 75%) in addition at the baffles, the temperature at the top of the targets, where T_{max} is located, decreases even further.

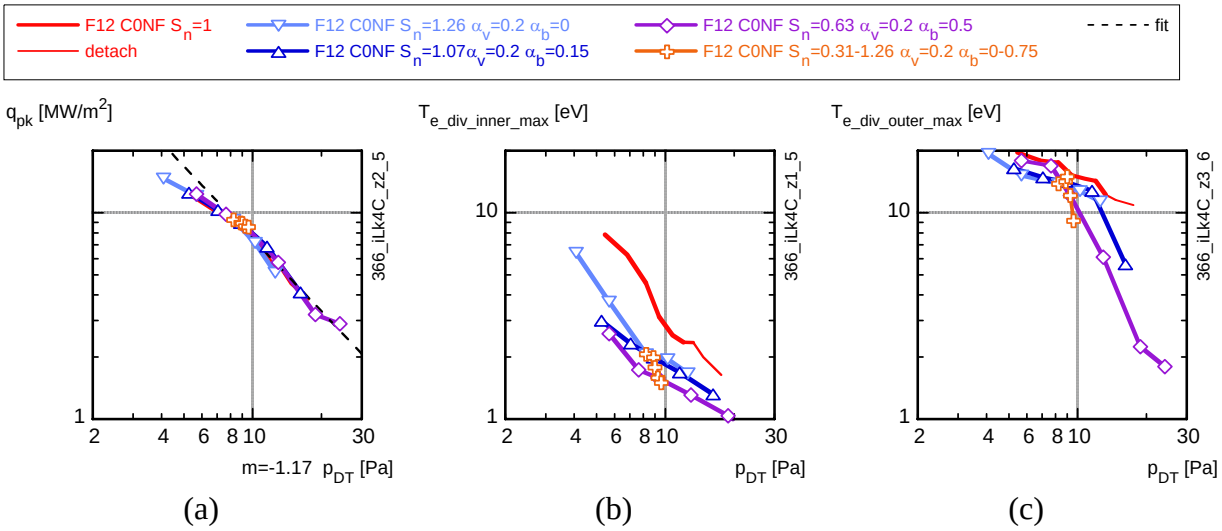

Fig. 2. Peak power (a) and maximum electron temperature in the inner (b) and outer (c) divertor vs. p_{DT} for different values of the particle reflux fraction α_b. Two exploratory series of runs where one of α_b, α_v was varied whereas the other and the total D content in the model were kept constant are also shown. When shown, "m" gives the fit exponent.

The effect of the particle reflux on the core interface parameters is shown in Fig. 3. Here the average ion density at, and the neutral influx into the core through, the separatrix are shown for D (fuelling) and He (helium removal). For D, both the ion density at the separatrix and the neutral influx to the core increase slightly, mostly because the throughput (and therefore the fuelling) increases for the same p_{DT} and therefore the recycling in the main chamber increases also.

To facilitate the assessment of the influence of the gaps, we introduce an effective engineering pumping speed which is proportional to the particle absorption fraction ξ as specified in the model times the absorbing area [3], corrected for the particle reflux fraction. This is obtained as follows. Pumping is given by an absorption ξ_d at the pump duct, pumping through the "V"s by an absorption ξ_v, and the particle reflux is characterised by α_b. Using Eq. (1), one can combine these parameters to get the pumping speed in presence of the gas leaks in the divertor structures, normalised to the value without these:

$$S_n \equiv S_p / S_d = \left(1 + \frac{A_v \xi_v}{A_d \xi_d}\right)(1-\alpha_b) = \frac{1-\alpha_b}{1-\alpha_v} \qquad (2)$$

Here S_p is the effective pumping speed relating the total throughput to the pump to the neutral

pressure in the divertor (if the latter were uniform and the neutral temperature were standard room temperature), S_d is the nominal pumping speed at the duct entrance.

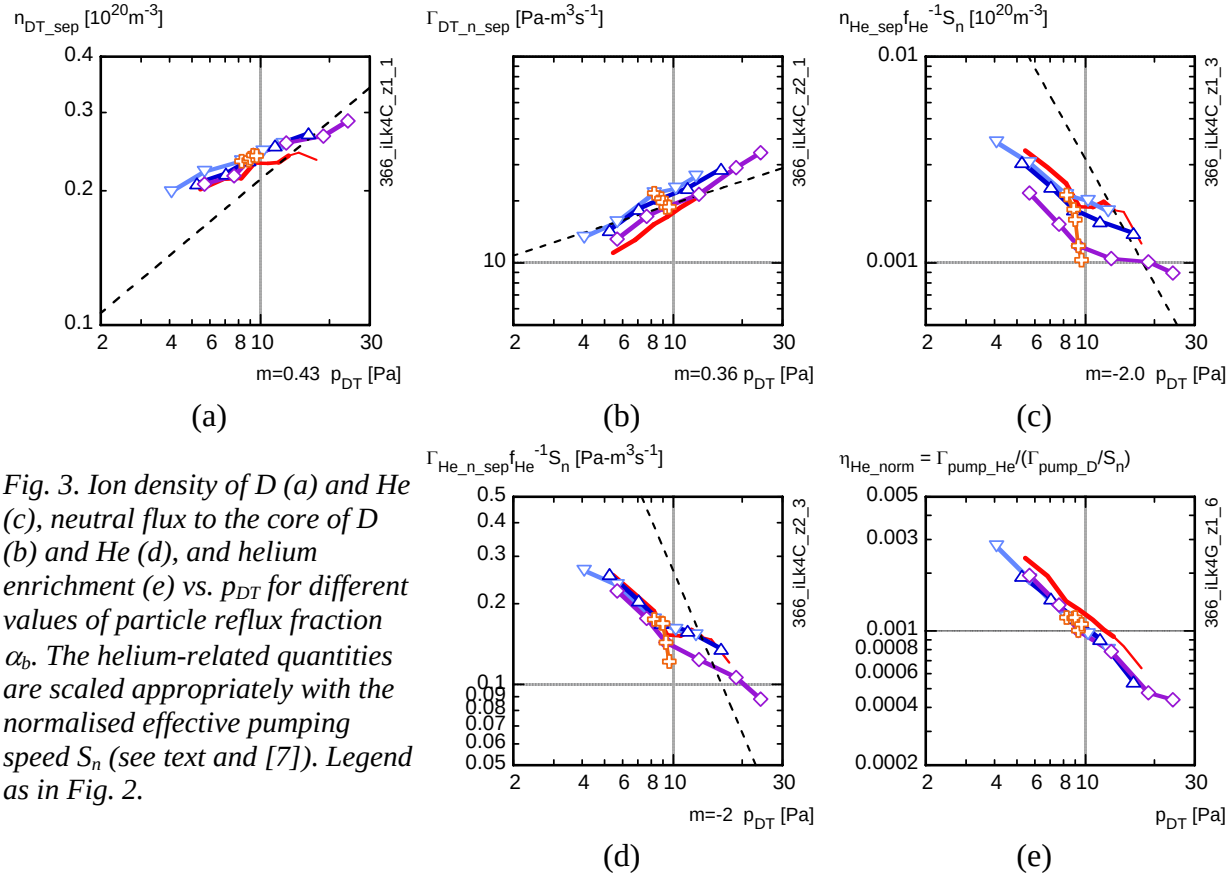

Fig. 3. Ion density of D (a) and He (c), neutral flux to the core of D (b) and He (d), and helium enrichment (e) vs. p_{DT} for different values of particle reflux fraction α_b. The helium-related quantities are scaled appropriately with the normalised effective pumping speed S_n (see text and [7]). Legend as in Fig. 2.

The helium-related quantities in Fig. 3 are scaled with this effective engineering pumping speed S_n because, in the absence of profile effects, at equal helium production rate and therefore throughput, the helium related quantities should be inversely proportional to the pumping speed, and previous studies [7] have confirmed that this remains the major effect for the complete calculation. Indeed, this continues to hold for the present results: whereas the He neutral flux is quite different for cases with and without leaks at the V's and/or reflux, it superposes well when scaled with S_n (Fig. 3d). The scaled helium density at the separatrix, n_{He_sep}, however, decreases with reflux, Fig. 3c, which appears counter-intuitive at first. This becomes understandable if one considers a qualitative picture of helium flows in the SOL and divertor [8, 7] as shown in Fig. 4. The thermal force impedes the helium ion flow along the inner, hotter part of the SOL, so that it reaches the targets mostly further outside the separatrix. Since the helium-helium interactions are insignificant for the transport, the problem becomes linear and the helium density profile can be represented as a sum of two components corresponding to different sources: one from the fusion production in the core, another from the reflux. The reflux component contributes less to the separatrix density since the bulk of the neutral influx is ionized in the outer SOL where the ions can flow back to the targets, and this additional source is compensated in the model

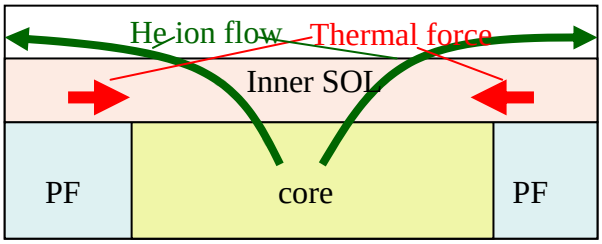

Fig. 4. Schematics of helium flows in the SOL and divertor region (unfolded on a rectangular area). Left and right edges represent the targets, upper edge the outer wall.

by increased pumping in the PFR ($\Gamma_p = \Gamma_c$ for He). Therefore re-direction of some part of the helium throughput at the divertor bottom to the reflux channel should cause a reduction of n_{He_sep}, as we see in our calculations. The helium enrichment at given p_{DT}, helium production rate, and pumping speed (Fig. 3e) is lower by ~30% in the presence of the gaps (equivalent to a higher required DT fuelling at constant He production rate by the same amount). Working at the same enrichment would require a ~20% lower p_{DT}, undesirable because of the increase of power load and helium density then.

The effects of the leaks are therefore either relatively small (peak power load, helium flux, DT neutral flux to the core, helium enrichment) or beneficial (helium ion density).

4. Sensitivity to the Target Shape

Since no negative effect of the gas leaks around the divertor corners were found (previous section), and these leaks should affect the tightness of the "V"s, it is natural to re-assess the role of the latter in the divertor performance in view of the improved model of the neutral particle transport. In order to do this, we consider four different modifications of the divertor shape, as shown in Fig. 5, ranging from very open corners (F31) to the deep "V" (F34).

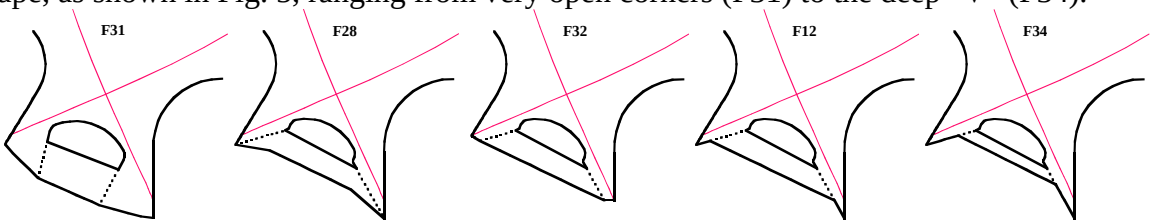

Fig. 5. Variation of divertor geometry used in the re-exploration on the effect of the "V-shapes" near the separatrix strike points. F12 marks our standard modelling configuration, F28, F31, and F32 are more open, and F34 more tight. Dotted lines indicate partially transparent surfaces at the entrance to the PFR.

The result is illustrated in Fig. 6. We see no significant difference in the parameters determining the core fuelling ($\Gamma_{DT\_n\_sep}$, n_{DT_sep}), or the helium removal (n_{He_sep}, $\Gamma_{He\_n\_sep}$). The target power load (q_{pk}) can decrease somewhat, but only by less than 40%, and this can be compensated by ~ 20% increase of p_{DT}.

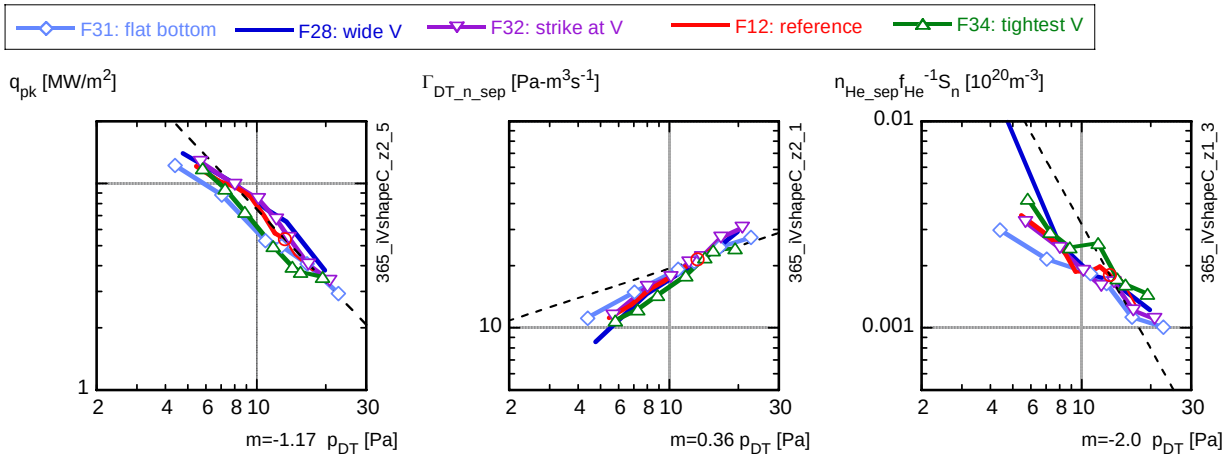

Fig. 6. Peak power (a), D neutral influx into the core (b) and He ion density at the separatrix (c) vs. p_{DT} for different shapes of the divertor bottom (see Fig. 5). S_n = 0.83 for F32 and 1 for the rest.

This relative insensitivity to geometry differs from previous studies [9] which used the linear neutral transport model that took into account neither neutral-neutral collisions nor collisions

of molecules with plasma ions. Therefore the neutral particles leaving the plasma travelled freely in the PFR, and their trajectories were determined solely by collisions with the solid surfaces. So the shape of these surfaces (not p_{DT}!) played an important role in the transport of neutrals. With the present model, the neutrals are scattered in the neutral-neutral collisions, and their mean-free-path is around 1 cm for typical pressures. As a result, they do not "feel" the shape of the divertor structures provided that the p_{DT} is the same, and therefore the effect of geometry changes is much smaller with this more complete model.

5. Sensitivity to the strike-point position

The positions of the separatrix strike-points on the divertor targets can only be kept with certain accuracy, and higher accuracy makes the demands on the control system more severe. The studies shown in the previous section (progression from F12 to F32) indicate that a shift of the strike-points towards the floor of the PFR would not affect the divertor performance significantly; this shift is only limited by the heat load on the dome. To explore the effect of the upward shift of the strike-points, we selected three configurations including the reference geometry, Fig. 7. The shifted configurations were in fact produced by keeping the same plasma equilibrium and shifting the divertor down by 12 and 24 cm (F21 and F20, respectively). Therefore the geometry of the SOL remains the same, and the results should show the effect of the variation of the divertor geometry.

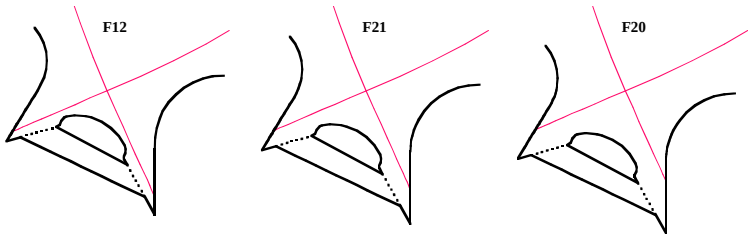

Fig. 7. Variation of the separatrix strike-point position on the targets used in the exploration. F12 is the reference geometry; F21 corresponds to the upward shift by 12 and F20 by 24 cm.

The results are shown in Fig. 8. As for the divertor shape variation, no significant difference in the performance parameters is seen, other than a slight (~ 20%) shift of the operational window to lower neutral pressure for the F20 geometry and a 20% increase in the separatrix DT density. To describe the results at the same operating point relative to divertor detachment, we therefore use a normalised value of the neutral pressure, $p_{DT}^{*} = p_{DT}\, f_s^{-1}$, where $f_s = 0.78$ for F20 and 1 for the other geometries considered. With this normalisation,

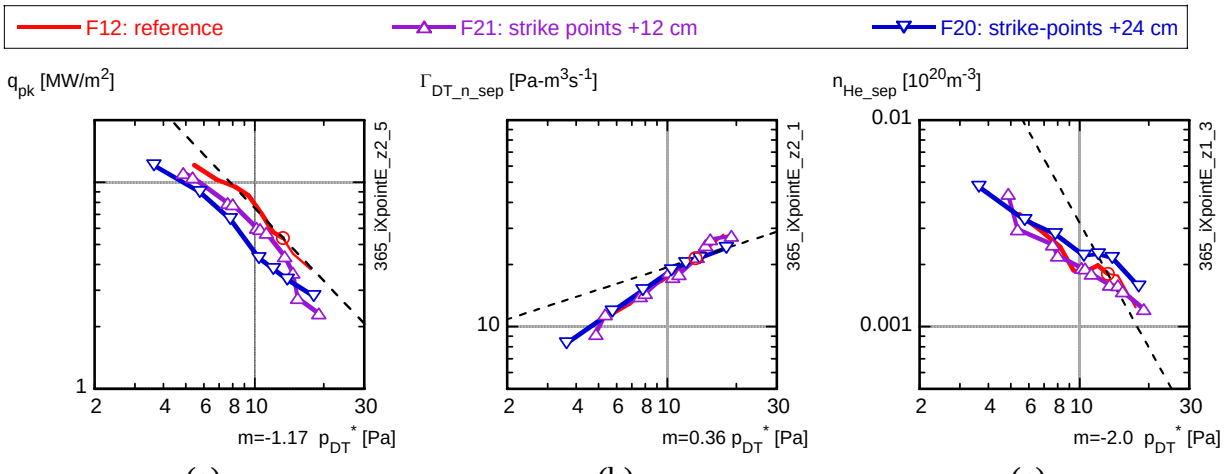

Fig. 8. Peak power (a), D neutral influx into the core (b) and He ion density at the separatrix (c) vs. normalised pressure in PFR, p_{DT}^{*}, for different positions of the separatrix strike-points on the targets (see Fig. 7).

the operational parameters for all three geometries follow similar curves, Fig. 8, except for a slight increase in n_{He_sep} in F20 – the helium neutralisation zone on the targets (see Fig. 4) becomes here well screened from the pump duct and this impedes He pumping.

7. Mid-plane gas puff

In another exploration of modification of the gas recirculation pattern in the edge, we study the effect of moving the location of the gas puff from the top of the machine to the outer mid-plane (OMP). One might naively expect the latter case to have much higher fuelling efficiency for the core plasma since the SOL in the OMP is almost an order of magnitude narrower than at the top (the second x-point is close to the first wall in ITER). However, our calculations show that this is not the case.

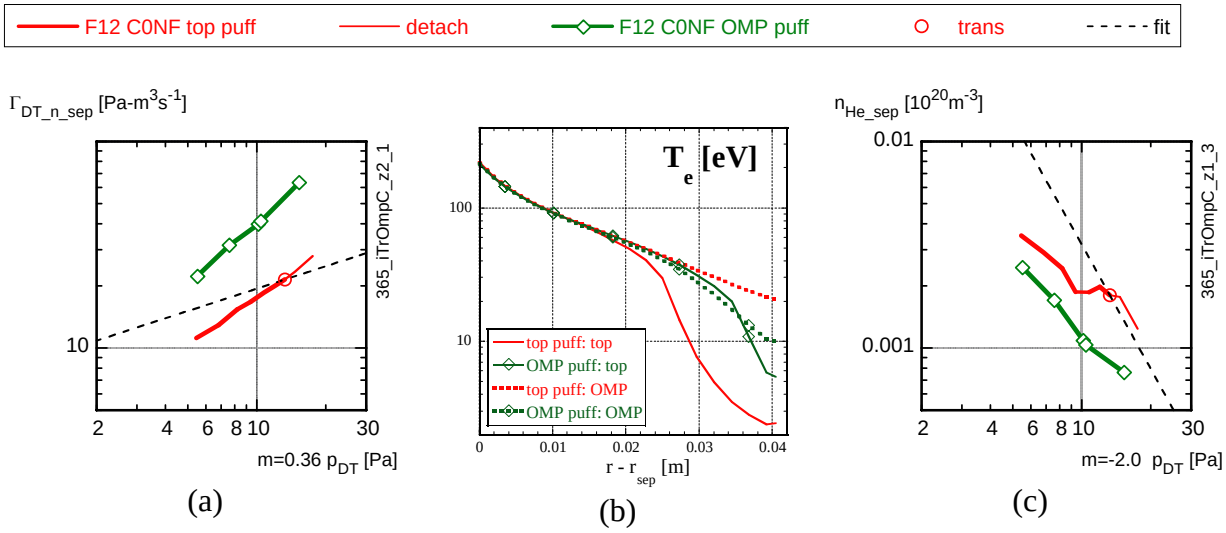

Fig. 9. Influx of D neutrals into the core (core fuelling rate) (a) and helium ion density at the separatrix (c) vs. p_{DT} for different locations of the gas puff, and radial profiles of the electron temperature (b) (mapped along magnetic field to the OMP) at the top and OMP.

Fig. 9a compares the neutral flux to the core for the two puff locations. One can see a rather moderate (a factor 2 to 3) increase of the fuelling efficiency when the gas is puffed from the OMP, which would still not suffice to fuel the central plasma of ITER by gas puffing alone [10]. The increase remains moderate for the following reason. Since the second x-point is close to the first wall, the magnetic pitch angle at the top of the chamber is small, so that for top puffing the parallel heat transport is not sufficient to maintain a constant temperature when the gas is puffed there. As a result, a cool plasma region forms in front of the gas injector, Fig. 8b, and the neutral penetration for top puffing is better than one might have expected. The density profiles in front of the puffing slots are similar, and the q_{pk} does not change for the same p_{DT}. For the OMP puff, the mid-plane ion temperature decreases by about 10% at the OMP puff location, and this explains the reduction of the helium ion density at the separatrix, Fig. 9c. Indeed, the thermal force balances the He pressure gradient when $n_{MP}/n_{div} \sim (T_{MP}/T_{div})^{3.5}$ [8]. Since T_{div} and n_{div} do not change, a 10% reduction of T_{MP} gives rise to a 50% reduction in n_{MP}. The reduction of n_{He} by a factor 2 is beneficial, but it is accompanied with an increased bombardment of the gas inlet area by energetic charge exchange neutrals (which may dominate non-carbon erosion, unlike in the present results).

7. Conclusions

We have further developed the computational model of the edge plasma in ITER, taking into account particle leaks through the gaps between the divertor cassettes. First results indicate no

major negative effect of the gaps on the divertor performance, although the parasitic flows caused by these gaps can be comparable with the pumping throughput. In the presence of the leaks, the dependence on the neutral gas pressure in the divertor of the peak power load on the targets remains unchanged and the core fuelling efficiency remains the same. The helium density at the separatrix decreases when the gaps are present because, at the same pumping speed at the pump, a fraction of the helium flux from the PFR is redirected to the baffle area via the leaks and contributes less to the helium density build-up at the separatrix. However, the helium enrichment decreases by 30%, i.e. the DT throughput is larger by this amount at the same helium production rate. On balance, since the presently assumed values (α_v =0.2, α_b =0.5) are representative of 12 mm gaps, larger than the 5 mm design value, and the effects are relatively small, sealing the inter-cassette gaps in ITER may not be a high priority issue.

The calculations reported in this paper confirm our previous observation [3] that the more comprehensive, non-linear model of the transport of the neutral particles [2] leads to much weaker sensitivity of the results to the details of the divertor geometry. In particular, it is not as important to maintain tightly sealed, pronounced V-shapes at the corners of the divertor targets close to the separatrix strike points as had been suggested earlier on the basis of the linear neutral model [9] because these geometric effects are attenuated by neutral-neutral collisions. This increases the flexibility, facilitating optimisation of both the divertor design and the plasma configuration in ITER. A deviation of the separatrix strike-points on the targets from their nominal positions by 20 cm upward is found tolerable, and their downward deviation is determined by the heat load on the dome, not by the divertor performance.

The gain in the core fuelling efficiency by changing the location of the main gas puff from the top to the outer mid-plane would be a factor 2 to 3, still insufficient to provide the required core fuelling by gas puffing alone. The decision is a trade-off between, on the one hand, the improvement of core fuelling efficiency (factor 2-3) and helium removal (factor 2) and on the other, likely increased wall erosion by energetic charge exchange neutrals near the mid-plane puffing location. Further dedicated modelling is needed to quantify these effects.

Further systematic work is needed and will be done to augment these observations. In particular, the effect of gas leaks through the divertor dome should be considered, together with a possible effect of the leaks on the gas pressure inside the divertor cassettes and so on the pumping efficiency, before the final recommendation on inter-cassette sealing can be given. Studies on adding seeded impurities have started (concentrations yielding an increase if impurity radiation by 4% so far); their continuation will be an important topic for future studies.

This report was prepared as an account of work undertaken within the framework of ITER Transitional Arrangements (ITA). These are conducted by the Participants: China, the European Atomic Energy Community, India, Japan, Korea, the Russian Federation, and the United States of America, under the auspices of the International Atomic Energy Agency. The views and opinions expressed herein do not necessarily reflect those of the Participants to the ITA, the IAEA or any agency thereof. Dissemination of the information in this paper is governed by the applicable terms of the former ITER EDA Agreement.

[1] G. Janeschitz, A. Antipenkov, G. Federici, et al., *Nucl. Fusion* **42** (2002) 14.
[2] A.S. Kukushkin, H.D. Pacher, V. Kotov, et al., *Nucl. Fusion* **45** (2005) 608.
[3] A.S. Kukushkin, H.D. Pacher, et al., 17th PSI, Hefei, 2006 (to appear in *J. Nucl. Mater*.)
[4] C. Lowry, private communication.
[5] W. Steckelmacher, *J. Phys. D: Appl. Phys*. **11** (1978) 473.
[6] H.D. Pacher, A.S. Kukushkin, et al., 17th PSI, Hefei, 2006 (to appear in *J. Nucl. Mater*.)
[7] A.S. Kukushkin, H.D. Pacher, G.W. Pacher, et al., *Nucl. Fusion* **43** (2003) 716.
[8] S.I. Krasheninnikov, A.S. Kukushkin, T.K. Soboleva, *Nucl. Fusion* **31** (1991) 1455.
[9] A. S. Kukushkin, H. D. Pacher, *Plasma Phys. Control. Fusion* **44** (2002) 931.
[10] G.W. Pacher, H. D. Pacher, et al., *Plasma Phys. Contr. Fusion* **46** (2004) A257.